Rome 1995 XXIV ICRC SH 8.1.13, Vol. 4

Differential Flux Measurement of Atmospheric Pion, Muon, Electron and Positron Energy Spectra at Balloon Altitudes

C. Grimani[1], P. Papini[2], S.A. Stephens[3], G. Basini[4], F. Bongiorno[4], F. Massimo Brancaccio[2], M.T. Brunetti[1], A. Codino[1], N. Finetti [2 1], R.L. Golden[5], M. Hof[6], M. Menichelli[1], J.W. Mitchell[7], A. Morselli[8], J.F. Ormes[7], M.P. De Pascale[8], C. Pfeifer[6], S. Piccardi[2], P. Picozza[8], M. Ricci[4], I. Salvatori[1], M. Simon[6], P. Spillantini[2], S.J. Stochaj[5], R.E. Streitmatter[7]

[1]*Università di Perugia and INFN, Perugia, Italy.* [2]*Università di Firenze and INFN, Firenze, Italy.* [3]*Tata Institute of Fundamental Research, Bombay, India.* [4]*I.N.F.N.-Laboratori Nazionali di Frascati, Frascati, Italy.* [5]*Particle Astrophysics Lab, New Mexico State University, Las Cruces, USA.* [6]*Universität Siegen, Fachbereich Physik, Siegen, Germany.* [7]*NASA Goddard Space Flight Center, Maryland, USA.* [8]*Università di Roma "Tor Vergata" and INFN, Rome, Italy.*

Abstract

The fluxes of atmospheric electrons, positrons, positive and negative muons and negative pions have been determined using the NMSU WiZard-MASS2 balloon-borne instrument. The instrument was launched from Fort Sumner, New Mexico, (geomagnetic cut-off of about 4.5 GV/c) on September 23, 1991. The flight lasted 9.8 hours and remained above 100,000 ft. Muons and negative pions were observed and their momenta were determined. Since these particles are not a part of the primary component, the measurement of their fluxes provides information regarding production and propagation of secondary particles in the atmosphere. Similarly, observations of electrons and positrons well below the geomagnetic cut-off provides insight into electromagnetic cascade processes in the upper atmosphere. In addition, the determination of the energy spectra of rare particles such as positrons can be used for background subtraction for cosmic ray experiments gathering data below a few g/cm^2 of overlying atmosphere.

1 Introduction

Galactic cosmic rays diffusing towards the Earth are deflected by the geomagnetic field. No primary cosmic rays reach the top of the atmosphere below a typical value of the cut-off rigidity characteristic of each site on the Earth. Cosmic rays observed at balloon altitudes below the cut-off are generated by higher energy particle interactions in atmosphere. The measurement of particle fluxes at a few g/cm^2 of atmospheric depth permits cascade calculations to be checked. Moreover, the knowledge of the atmospheric component is needed for background subtraction in the measurements of rare particles, such as positrons, made with balloon-borne experiments.

2 Apparatus and Data Analysis

The MASS2 experiment consisted of the following devices: a time-of-flight scintillator system (TOF), a gas Cherenkov detector (G), a superconducting magnet spectrometer and a streamer tube imaging calorimeter (C). The TOF consisted of 3 planes of plastic scintillator paddles located at the top of the instrument and below the chamber stack. The TOS is used to determine the particle's velocity. A TOF resolution of few hundreds ps assures an up-down rejection at more than 30 standard deviations. The G detector was filled with Freon 12 giving a threshold Lorentz factor of 23.5. The spectrometer consisted of a superconducting magnet and a hybrid system of 8 MWPCs and two modules of drift chambers. The magnet generated a maximum magnetic field of 2.2 T in the chamber region. The spectrometer MDR was 210 GV/c. The imaging calorimeter consisted of 40 planes of 64 brass streamer tubes each, for a total of 7.3 radiation lengths and 0.75 nuclear interaction lengths. The calorimeter permitted the topological reconstruction of the particle interactions. The secondary electron and positron differential fluxes were determined between 300 MeV/c and 4 GeV/c while pions and muons between 5 and 15 GeV/c and 250 MeV/c and 20 GeV/c respectively. The particle selection criteria are

shown in Table 1. Test 1, Test 2, Test 3 and Test 4 give a reliable deflection determination in the magnetic spectrometer. Test 5 permits the selection of minimum ionizing particles from the total sample of events, Io being the expected pulse-height corresponding to a minimum ionizing particle and T1 and T2 the average of the top and bottom scintillator charge measurements. Test 6 and Test 6a verify whether or not that a Cherenkov signal has been generated. The average number of photoelectrons generated by a fully relativistic particle was about 18. Test 7 is an energy dependent criterion for particle selection in the calorimeter, see [?] for shower-cluster (s-c) definition. A high number of shower-clusters is characteristic of a high multiplicity, collimated electromagnetic shower. On the other hand, a small number of shower-clusters is related to a low multiplicity, high opening angle hadronic shower. Non-interacting particles should not generate shower-clusters. Tests 7 were used above 1 GeV since no reliable shower identification can be made in the calorimeter for low energy particles generating a small number of secondaries. Since pions have to be separated from the bulk of the other negative particles, mainly electrons and muons, we selected interacting pions only; the number of shower-clusters generated by hadronic interactions and the shower opening angle were found to be very powerful tools. Below 2 GeV, good particle separation was obtained by using the particle square masses as a function of beta (see Papini et al., presented at this conference).

Table 1: *Electron, Positron, Pion and Muon Selection Criteria*

Test1. At least 11 chambers in the direction of the maximum bending of the magnet (x-view) and 6 in the orthogonal direction (y-view) give a good signal. **Test2.** The least-square fit ot the reconstructed track must have $\chi_x^2 \leq 8$ and $\chi_y^2 \leq 8$. **Test3.** The number of drift chamber planes with hits at more than 4 cm from track has to be less than 3 in both views. **Test4.** The uncertainty in deflection has to be less or equal to 0.03.
Test5. $Z_{T1} \leq 1.8 Io$ and $Z_{T2} \leq 1.8 Io$
Test6. Cherenkov pulse-height $\geq$ 1. photoelectron.
Test6a. Cherenkov pulse-height $\leq$ 1. photoelectron
Test7a. Electrons and positrons 1 - 2 GeV/c: A minimum of 2 calorimeter planes show s-c in, at least, one calorimeter view. 2 - 4 GeV/c: A minimum of 4 calorimeter planes show s-c in, at least, one calorimeter view.
Test7b.Pions The maximum number of s-c shown by the calorimeter views is greater than 4 and smaller than 12. The shower opening angle in the calorimeter has to be at least 25 degrees.
Test7c.Muons No more than one plane, in both calorimeter views, shows s-c

3 Results and Discussion

The geometrical factor, the experiment live time and the efficiencies of the apparatus have been taken into account for particle absolute flux determination. The geometrical factor for low energy particles ranged from 232 cm^2 sr to 284 cm^2 sr while, when the calorimeter was included for selection, the geometrical factor was 167 cm^2 sr. The spectrometer and scintillator efficiencies were .93±0.03 and .85±0.06 respectively. The calorimeter efficiency was 1 for Test 7a between 1 and 2 GeV and .98 above 2 GeV, it was .64 for Test 7b and .93 for Test 7c. The flight lasted 35330 s with a dead time of 36%. Before flux determination the total number of pions was calculated from the observed interacting events and the contribution of non-interacting pions was subtracted from the muon flux. In Figures 1 and 2 we have reported the particle differential fluxes measured by this experiment for electrons, positrons, positive and negative muons and negative pions. Previous measurements made at different atmospheric depths [?, ?] have been reported also along with calculations [?]. A good agreement is observed with the theoretical expectations. It may be noted that just below the geomagnetic cut-off energy, one needs to consider the ranging down of primary particles due to energy loss processes and hadronic interactions, which would make these particles appear as secondaries.

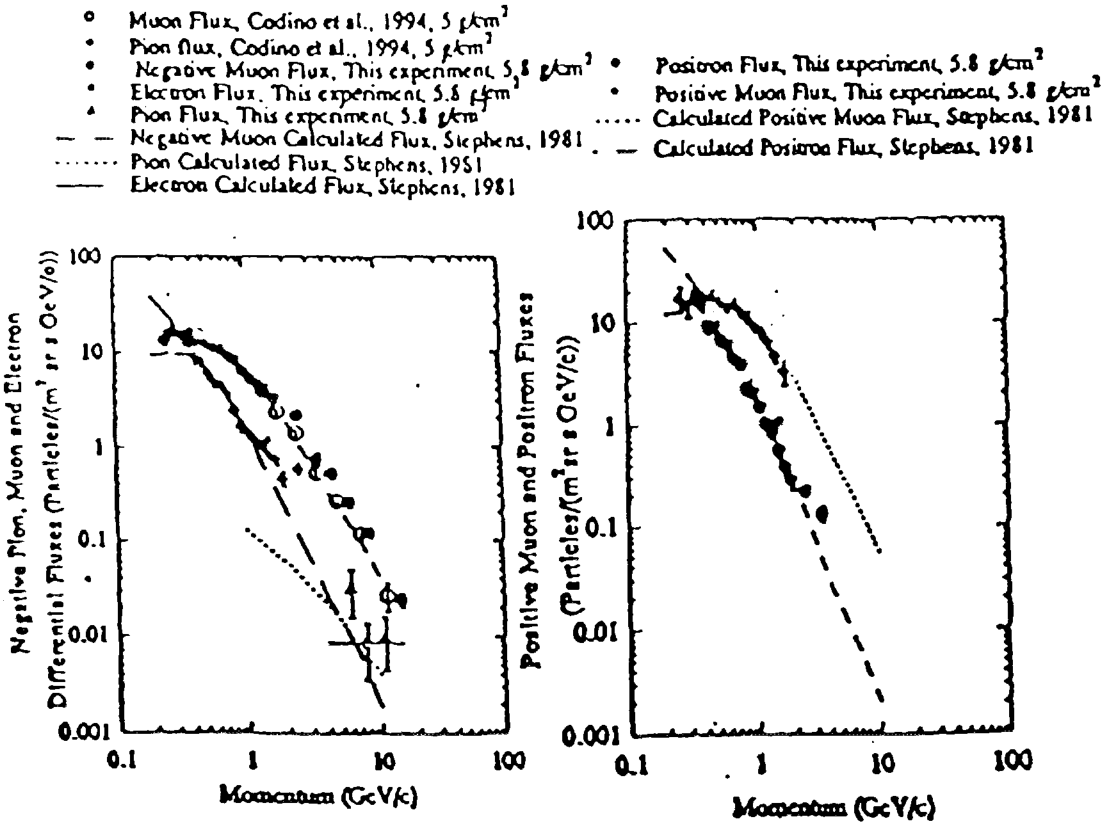

Figure 1: *Negative atmospheric particle fluxes*

Figure 2: *Positive atmospheric particle fluxes*

Acknowledgements. This work was supported by NASA, Grant NAG-110, the National Scientific Balloon Facility, USA, the Istituto Nazionale di Fisica Nucleare and the Agenzia Spaziale Italiana, Italy and the German Space Agency DARA, Germany.

References

[1] Golden R. L. et al., Ap. J., 436 (1994) 769

[2] Grimani C. et al., 23rd ICRC, Calgary, 4 (1993) 507

[3] Codino A. et al., Conf. Pap. Vulcano Workshop, Nuovo Cimento, (1995)

[4] Stephens, S. A., , 17th ICRC, Paris, 4 (1981) 282